MIT Open Access Articles

Effect of filler mass and binding on thermal conductivity of fully filled skutterudites

Effect of filler mass and binding on thermal conductivity of fully filled skutterudites

Mona Zebarjadi,[1] Keivan Esfarjani,[1] Jian Yang,[2] Z. F. Ren,[2] and Gang Chen[1,*]

[1]*Mechanical Engineering Department, Massachusetts Institute of Technology, Cambridge, Massachusetts 02139, USA*
[2]*Department of Physics, Boston College, Chestnut Hill, Massachusetts 02467, USA*

The relations between the thermal conductivity of cagelike structures and their crystal parameters are investigated using a two-dimensional toy model. The model consists of host atoms on a rectangular lattice with fillers at the center of each rectangle. The effect of mass and size of the filler on thermal conductivity is investigated using equilibrium molecular-dynamics simulations. We show that the thermal conductivity decreases with increasing atomic displacement parameter while it has local minima versus the filler to host mass ratio. Similar trends were observed in experiments on filled skutterudites. The trends are explained by analyzing the effect of the filler on the phonon dispersion and relaxation times of the host material.

I. INTRODUCTION

Skutterudites are one of the main classes of cagelike structures, which have been investigated largely for thermoelectric applications.[1–4] Their structure is composed of eight corner-sharing XY_6 (X=Co, Rh, Ir; Y=P, As, Sb) octahedra. The linked octahedra produce a void at the center of the $(XY_6)_8$ unit, where the void space occupies a body-centered position of the cubic lattice. The void is large enough to accommodate other atoms to form filled skutterudites. Filled skutterudites were first made and their crystallographic properties were investigated by Jeitschko and co-workers.[5,6] They reported large thermal vibrations of filler atoms. Slack[7] then pointed out that the introduction of such filler atoms can be an effective method to reduce the thermal conductivity because the "rattling" atom will strongly scatter the propagating phonons, which are responsible for most of the heat transport. The rattling picture is widely used for these materials. However, the rattling-induced phonon scattering in filled skutterudites has not been proven.[8] The rattling behavior is associated with a weak bonding of the filler to the cage, introducing the possibility of an independent, noncorrelated vibration of the filling atoms.[4,9] The first evidence of such localized modes, was reported by Keppens *et al.*[10] using heat capacity, elastic constant and inelastic neutron-scattering measurements. They were able to explain their heat-capacity data with the Debye model plus two fitted Einstein oscillators. Recently there have been debates on this picture. It has been pointed out by a higher resolution neutron scattering that the previously observed peaks were due to van Hove singularities, that is, optical phonons and zone boundary modes. According to this new observation, vibration modes of fillers are coherently coupled with the host phonons.[11]

In another approach for thermal conductivity calculations, partially filled skutterudites were accepted as solid solutions of completely filled and unfilled end members.[12] In this picture, the chemical disorder in the occupancy of the transition-metal sites is the main mechanisms for the reduction in thermal conductivity.[13]

In this work, we introduce a simple model, which was developed to help us understand the relationship between the thermal conductivity of cagelike structures and their crystal-structure parameters. The aim is to distinguish between the contributions of different types of atoms, when one type is strongly interacting while the other is weakly bounded. Two important parameters will be discussed: atomic displacement parameter and mass ratio of the filler to the cage. It has been observed experimentally that the thermal conductivity is largely reduced as the atomic-displacement parameter increases. We further show that, as a function of mass ratio there is a minimum in the thermal conductivity. We think that these features are universal and confirm our claim by showing that the features are observable even in a simple two-dimensional (2D) model

II. MODEL

The model consists of a two-dimensional rectangular centered lattice as indicated in Fig. 1. The primitive cell of this structure is a rectangle with host atoms sitting at the corners and filler atoms at the center. The aspect ratio of $1/\sqrt{3}$ is chosen for the rectangle to form a stable close packed triangular structure with six nearest neighbors. Host atoms have a Lennard-Jones (LJ) interaction. The fillers are placed such that their equilibrium position is at the center of host rectangles. Each filler is connected to its cage (host atoms sitting on the rectangle around it) by four identical springs with interactions of the form $\phi_{ij}=\frac{1}{2}K(|\vec{r}_{ij}|-r_{eq})^2$ where K is the spring constant and r_{eq} is the equilibrium distance between atom pairs i and j. A weak filler-filler LJ interaction was also
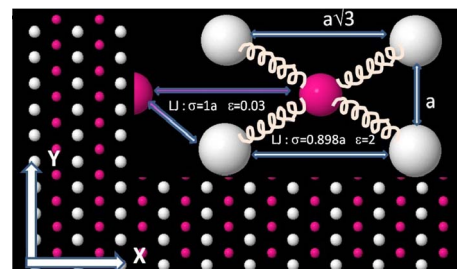

FIG. 1. (Color online) 2D lattice structure. White atoms are host atoms with LJ interactions. Each filler (pink atoms) is connected to its four nearest-neighbor host atoms by four identical springs.

introduced to avoid the structure from deforming. This is schematically shown in Fig. 1. Note that all the introduced interactions are anharmonic. The constructed model is one of the simplest possible cage structures. If the observed experimental trends are universal, we should be able to see the same trends even with the simplest model. The dimensionality is not an issue here since the aim is not to look at the scaling but rather we fix the size of the sample and just change relevant parameters (mass and spring constant). When dealing with 2D structures, there are usually concerns about localization and van Hove singularities, which might affect transport properties. Since there is no randomness in the current model, only fully filled and not partially filled structures are considered, localization is not expected to occur. Moreover, since the modeling is at finite temperature and because of the considered anharmonic potential, van Hove singularities are smeared out and do not affect the transport properties.

We use equilibrium molecular-dynamics (MD) simulations to calculate thermal properties of the structure. The output thermal currents of the molecular dynamics are used to calculate the thermal conductivity with the Green-Kubo formalism

$$\kappa^{\alpha\beta} = \frac{1}{AK_BT^2}\int_0^\infty \langle j^\alpha(0)j^\beta(t)\rangle dt, \quad (1)$$

$$\vec{j}(t) = \sum_i \vec{v}_j\varepsilon_i + \frac{1}{2}\sum_{i,j,i\neq j}\vec{r}_{ij}(\vec{F}_{ij}\cdot\vec{v}_i), \quad (2)$$

$$\varepsilon_i = \frac{1}{2}m_i|\vec{v}_i|^2 + \frac{1}{2}\sum_j \phi_{ij}, \quad (3)$$

where $\kappa^{\alpha\beta}$ is the thermal conductivity tensor, A the area, K_B the Boltzmann constant, T the temperature, $\vec{j}(t)$ the heat current at time t, angular brackets denote the ensemble and time averaging, $\vec{v}_i$ the velocity, ε_i the site energy, $\vec{r}_i$ the position, and m the mass of the atom i, $\vec{F}_{ij}$ the force exerted by atom j on atom i, ϕ_{ij} the pair potential, and $\vec{r}_{ij}$ the vector connecting them.

Simulations were done for an 18×30 unit-cells lattice (1080 atoms). A set of arbitrary units were chosen since the aim was not to compare results with the experimental data quantitatively. In these units (length a_0, mass m_0, and time t_0), LJ interaction strength (ε) is set to $2\varepsilon_0$ ($\varepsilon_0=m_0a_0^2/t_0^2$) between host-host atoms and to $0.03\varepsilon_0$ between filler-filler atoms, temperature is set to $0.03\varepsilon_0/K_B$, neighboring interaction cutoff is $2.5a_0$, the MD time step is set to $0.2t_0$ (which is half of the maximum time step at which the structure is still stable). Before each run, the lattice is equilibrated with a Langevin thermostat. A microcanonical MD simulation is run for 500 000 steps. These runs are repeated with 100 different initial conditions in order to simulate an ensemble averaging. Long-time averaging is required to minimize the time averaging error bar. Ensemble averaging is used to sample the phase space. With these measures, the thermal conductivity can be calculated with less than 20% uncertainty.

Although the molecular-dynamics simulation gives the thermal conductivity, it is difficult to distinguish between the effects of phonon velocities and lifetimes. To do so, we have developed a lattice-dynamics simulation tool, which can calculate phonon dispersions within the harmonic approximation from the force constants between atom pairs.[14] Having phonon dispersions, group velocities can be calculated for each mode and at each q point in the reciprocal space. The thermal-conductivity component in $\alpha\beta$ directions can be written as

$$k^{\alpha\beta} = \frac{1}{n_qA}\sum_\lambda \sum_{q\,\in\,\text{FBZ}} \hbar\omega_\lambda(q)v_\lambda^\alpha(q)v_\lambda^\beta(q)\tau_\lambda(q)\frac{\partial n}{\partial T}$$

$$= \sum_\lambda \int_0^{\omega_{max}} d\omega\text{DOS}_\lambda(\omega)\hbar\omega_\lambda v_\lambda^\alpha(\omega)v_\lambda^\beta(\omega)\tau_\lambda(\omega)\frac{\partial n}{\partial T}, \quad (4)$$

where q is the wave vector, λ the mode index (branch index), v_λ^α the group velocity in the α direction for the λ mode, n the Bose-Einstein distribution function, n_q the number of q points sampling the first Brillouin zone (FBZ), $\text{DOS}_\lambda(\omega)$ the density of states per unit area per mode, A the primitive cell area, and τ the relaxation time. The only scattering mechanism in the current model is the phonon-phonon scattering which comes from the anharmonicity of the potential. The only source of resistance in this model is the three-phonon Umklapp scattering. This process can be approximated by Klemens' expression for anharmonic phonon scattering.[15]

$$\frac{1}{\tau_\lambda(q)} = \frac{2\gamma_\lambda^2(q)K_BT}{Mv_\lambda^2(q)}\frac{\omega_\lambda^2(q)}{\omega_{\lambda,max}}, \quad (5)$$

where γ_λ is the Grüneisen parameter, M the mass of the unit cell, and $\omega_{\lambda,max}$ the maximum frequency of branch λ. The Grüneisen parameter at each q and λ can be calculated from the change in the phonons' frequencies with the cell volume.

$$\gamma_\lambda(q) = -\frac{d[\ln\omega_\lambda(q)]}{d(\ln A)} = -\frac{\omega_{\lambda,l+\Delta l}(q) - \omega_{\lambda,l-\Delta l}(q)}{2\omega_{\lambda,l}(q)}\times\left(\frac{L}{2\Delta L}\right). \quad (6)$$

The importance of the Umklapp scattering effect in skutterudites due to the cubic anharmonic interaction between filler and host atoms, has recently been discussed by Bernstein *et al.*[16]

III. RESULTS AND DISCUSSION

A. Atomic-displacement parameter (ADP)

It is generally believed that the smaller and the heavier the ion in voids, the larger the reduction in the lattice thermal conductivity. Large cage sizes and small filler ions can have larger atomic-displacement parameters. Recently Matsuhira *et al.*[17] showed that the Einstein temperature decreases linearly (with few exceptions) as the cage size increases. Fleurial *et al.*[2] experimentally showed that the thermal conductivity decreases exponentially as the atomic-displacement parameter increases.[18] Sales *et al.*[19] were able to connect the
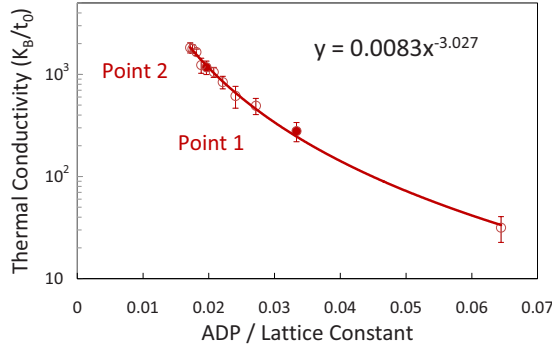
FIG. 2. (Color online) Average thermal conductivity (averaged over direction) versus atomic-displacement parameter of the filler. For this simulation the host mass was set to $40m_0$ and the filler mass to $12m_0$.

thermal conductivity to the atomic-displacement parameter with a phenomenological approach (Debye model+Einstein oscillators).In the current model, the atomic-displacement parameter can be changed by changing the spring constant of the connecting filler-host springs. The ADP parameter is defined for each atom as the square root of the variance in the position of the atom. We then average over all atoms of the same type: $ADP_i = \frac{1}{n_i} \sum_{j \in \text{type } i} \sqrt{\langle r_j^2 \rangle - \langle r_j \rangle^2}$, where r_j is the position of atom j, the averaging is over time, and the sum is over all atoms of type i in the simulated supercell.

The observed trend in Fig. 2 is very interesting since it is similar to the experimentally observed trend in filled skutterudites, despite the simplicity of our model (see Fig. 7 in Ref. 18). As the spring constant decreases, frequencies shift to lower values, resulting in lower group velocities of the acoustic bands of the lattice. The atomic-displacement parameter increases since bindings are weaker and atoms can move more freely. This in turn, results in stronger phonon-phonon scatterings and therefore shorter lifetimes. Both reductions in group velocities and lifetimes result in lower thermal conductivity. To see how much of the reduction is due to reduction in velocities and how much is due to lifetimes, consider two points on Fig. 2, the first point corresponds to an atomic-displacement parameter of $0.033a_0$ and a thermal conductivity of $278K_B/t_0$, and the second point corresponds to an ADP of $0.019a_0$ and a thermal conductivity of $1174K_B/t_0$ (These are labeled in Fig. 2). Using Eqs. (4) and (5), the thermal conductivity is recalculated taking the Grüneisen parameter as a fitting parameter.

Figure 3(a) shows the normalized frequency-dependent DOS, group velocity squared, and lifetimes for the second chosen point (corresponds to ADP of $0.019a_0$). (Note that the steps in the density of states are from the extrema of the phonon dispersion and the sharp peaks or van Hove singularities of the density of states are from the saddle points in the phonon dispersion) The main contribution to the thermal conductivity comes from low-frequency phonons. In fact 75% of thermal conductivity is from phonons with frequencies less than $0.5t_0^{-1}$. For the first chosen point (ADP of $0.033a_0$), the value increases to 95%. Figure 3(b) shows the ratio of the thermal conductivity, density of states, group velocity squared, and lifetimes versus frequency for the two
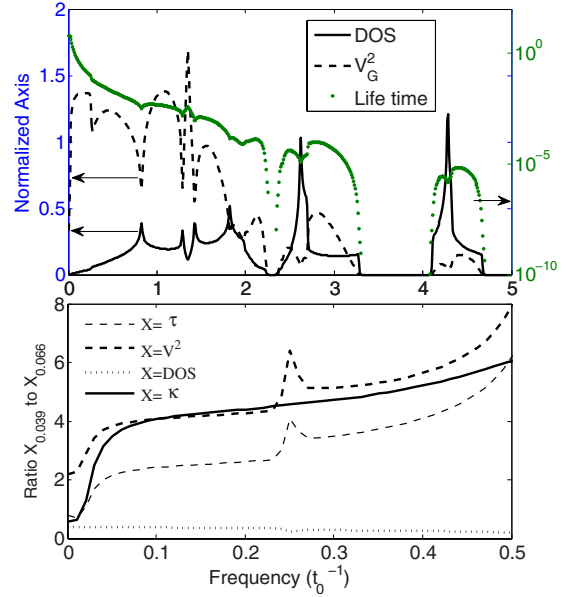
FIG. 3. (Color online) (top) Frequency dependence of normalized density of states, phonon lifetimes, and group velocity squared for atomic-displacement parameter of $0.039a_0$. (bottom) Ratio of lifetimes (τ), velocity squares, density of states, and thermal conductivity at two different points of Fig. 2 versus frequency (the numerator corresponds to ADP=$0.039a_0$ and the denominator corresponds to ADP=$0.066a_0$). This shows that as ADP is decreased, group velocities first, and relaxation times next, contribute to the increase in thermal conductivity.

chosen points at low frequencies. It can be seen that while at low frequencies the group velocities and relaxation times are, respectively, five and three times larger, the DOS is more than halved when the ADP is decreased. As a result, the contribution is mostly from the change in the velocities and also the relaxation times; while at high frequencies, the main contribution is from phonon lifetimes (this is not shown). Since the main contribution to the overall thermal conductivity is from low frequencies, one can conclude that overall the main cause of thermal conductivity reduction versus ADP is due to a reduction in group velocities.

B. Mass ratio

The mass ratio of the filler to the cage is another interesting parameter to look at. Higher filler mass corresponds to lower frequency modes and therefore is expected to reduce the thermal conductivity as it scatters lower phonon frequencies, which contribute more to the thermal conductivity. However, if we plot the experimentally measured thermal conductivity at room temperature versus the mass ratio of the filler to the host cage, we observe a minimum. Increase in the filler frequencies by increasing the filler mass is not expected but it has been reported in some cases,[20,21] which can be attributed to the difference in the binding strength of these ions. It has also been reported that in cobalt-based skutterudites, as one increases the cage mass, the thermal conductivity decreases. In Fig. 4, we report the experimental data of antimonite skutterudites samples, which were synthesized

FIG. 4. (Color online) Room-temperature lattice thermal conductivity of different filled skutterudites versus mass ratio of the filler to the cage (f_{filler} is the filling fraction). Squares are labels for Co_4Sb_{12} family of skutterudites, triangles for $Fe_3Co_1Sb_{12}$ and diamonds for $Fe_{3.5}Co_{0.5}Sb_{12}$. Fillers and their molar fractions are labeled on each data point. For example $Ba_{0.25}$ in the label of a red square data, refers to $Ba_{0.25}Co_4Sb_{12}$. Purple circles are data from the literature.[27–29] These are labeled individually with their names and references. The dashed line is just a guide to the eye.

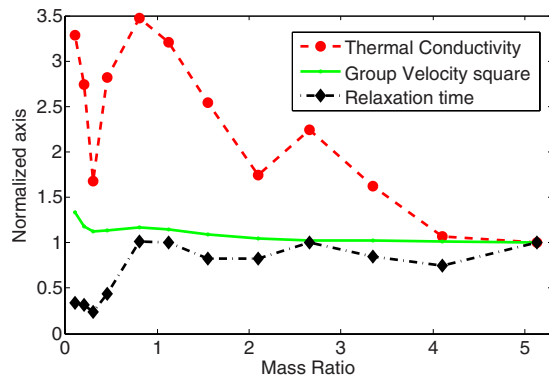and measured in this study as well as data for other types of skutterudites from the literature. The aim is to show the trend, rather than claiming that all of the experimental data on any type of skutterudites will fall on the same curve. The details of the synthesis and measurements are described in details in other publications.[22–26] The samples that are used in this plot are nanostructured samples. The grain sizes are quite large (more than 200 nm and larger than phonon mean-free path). Therefore, grains do not affect the phonon transport and nanostructuring effects can be ignored. The lattice thermal conductivity is extracted using the Wiedemann-Franz relation. Figure 4 shows that the experimental thermal conductivity has a minimum at about 0.07 versus mass ratio. To understand this behavior, we fix the host mass in our model and then scan the filler mass such that the mass ratio goes from zero to five. Figure 5 shows the resulting thermal conductivity in different directions. Note that the system is anisotropic. The thermal conductivity in the y direction is dominated by host atoms and in the x direction by fillers.

Figure 5 shows that the thermal conductivity versus mass ratio has local minima. This is consistent with the experimental data. Note that in the real experiment, it is not possible to go beyond the ratio of about 0.25, for filled skutterudites. To understand where the minima come from, we analyzed group velocities and relaxation times and recalculated the thermal conductivity from Eqs. (4)–(6). Let us focus on the first minimum, which is experimentally observable. We choose three points on Fig. 5 corresponding to mass ratios of 0.1, 0.3, and 0.8. These points are maximum, minimum, and maximum, respectively. For these three points, group velocities and lifetimes in the FBZ are plotted in Fig. 6. Due to symmetry, there are four equivalent parts in the FBZ. Since there are also four bands in the model, we showed each band in one quarter of the FBZ.

Fillers affect both phonon velocities and relaxation times. As we introduce fillers into the lattice, two optical bands are

FIG. 5. (Color online) Thermal conductivity of the lattice in x and y directions versus mass ratio. Spring constant of the filler-host is 5. The LJ potential of host-host can be fitted with an equivalent spring constant of 70. Therefore filler-host interaction is much weaker than host-host interaction. The thermal conductivity in a smaller mass ratio range (0:1) is also shown in the inset.

added to the system. All bands shift to lower frequencies as the mass of the filler increases. For acoustic bands, this means lower group velocities and therefore less contribution to the thermal conductivity (Fig. 6(a) bands 1 and 2). The optical bands are usually flat but when they come close enough to the acoustic bands of the host, they hybridize with them. The hybridization gives some features to the optical bands. They gain a finite slope and are more populated since they have shifted to lower frequencies, and so they start to contribute to the thermal conductivity (see Fig. 6(a) bands 2 and 3).

Fillers affect relaxation times as well. Fillers are scattering centers. Therefore adding fillers would increase scattering rates and reduce phonon relaxation times. The increase in the relaxation time [plotted in Figs. 6(b) and 7] with the mass

FIG. 6. (Color online) (a) Group velocities and (b) logarithm of relaxation times of Klemens' model in the FBZ. Each quarter of the FBZ is devoted to one band. Band numbers are labeled in the top left figure. G_1 and G_2 are the reciprocal wave vectors. The plots from left to right are for mass ratios of 0.1, 0.3, and 0.8, respectively. As the latter is increased, one can see an overall reduction in group velocities of acoustic branches (1 and 2 on top) and a large increase in their relaxation times.

FIG. 7. (Color online) Normalized (to mass ratio=5.1) thermal conductivity [Eq. (4)], group velocity in the x direction, and relaxation time [calculated from Klemens' model Eqs. (5) and (6)] versus mass ratio.

ratio may be understood in terms of the Fermi golden rule, which displays a decreasing scattering *rate* versus mass.

Since Klemens' expression for relaxation times is just a rough approximation, we were not able to reproduce the molecular-dynamics thermal conductivity of Fig. 5 from Eqs. (4)–(6) exactly. However, the Klemens' formula was able to produce main features of molecular dynamics data. Figure 7 shows the resulting normalized thermal conductivity in the y direction. The thermal conductivity is divided by 46.5 (thermal conductivity value at mass ratio of 5.1) in this figure. On the same figure we also show the average velocity squared ($\Sigma_{q,\lambda} v_{\lambda,q}^{y\ 2}$) and the average relaxation time [$\Sigma_{q,\lambda} \tau_\lambda(q)$] (averaged over all q points in the FBZ which are shown in Fig. 6). These are also scaled by their values at mass ratio of 5.1 so that we could show all three curves on the same plot. At the first minimum of the thermal conductivity, both velocity and relaxation time have a minimum; however, the minimum of relaxation time is deeper. One should note that relaxation times are not independent from velocities. Equation (5)

shows how relaxation times are related to phonon dispersions. The second minimum comes completely from relaxation times.

In summary, we simulated the behavior of thermal conductivity of filled skutterudites versus filler mean-square displacements and mass with a simple model. The Green-Kubo MD simulations of this model were also compared to Klemens' model results based on lattice dynamics and good qualitative agreement was found. Predictions of this model in terms of lowering of thermal conductivity versus filler mean displacements and a minimum versus mass ratio were also in agreement with experimental results on filled skutterudites. This can be taken as an indication of the universal nature of these trends. We further separated the contributions of group velocities and phonon lifetimes in the thermal conductivity. It was shown that the thermal conductivity behavior could be explained from the details of the full phonon dispersions without a need to introduce extra scatterings. The decay of the thermal conductivity versus atomic displacement parameter comes mainly from the reduction of group velocities as the binding strength of pair atom interaction decreases. In the general case where there is a minimum in the thermal conductivity versus the filler mass, the initial reduction in the thermal conductivity can be attributed to the lowering of acoustic phonons group velocity. The further increase in κ comes, in part from the increasing contribution of optical bands, and in part from the increase in relaxation times, as the mass ratio is increased (see Fig. 7).

ACKNOWLEDGMENTS

*gchen2@mit.edu.

[1] B. X. Chen, J. H. Xu, D. T. Morelli, G. P. Meisner, J. P. Fleurial, T.Caillat, and A. Borshchevsky, Phys. Rev. B **55**, 1476 (1997).

[2] J. P. Fleurial, T. Caillat, and A. Borshchevsky, in Proceedings of the 16th International Conference on Thermoelectrics (IEEE, Piscataway, NJ, (1997), pp. 1–11.

[3] G. S. Nolas, G. A. Slack, D. T. Morelli, T. M. Tritt, and A. C. Ehrlich, J. Appl. Phys. **79**, 4002 (1996).

[4] B. C. Sales, D. Mandrus, B. C. Chakoumakos, V. Keppens, and J. R. Thompson, Phys. Rev. B **56**, 15081 (1997).

[5] W. Jeitschko and D. Braun, Acta Crystallogr., Sect. B: Struct. Crystallogr. Cryst. Chem. **33**, 3401 (1977).

[6] D. J. Braun and W. Jeitschko, J. Less-Common Met. **72**, 147 (1980).

[7] G. A. Slack and V. G. Tsoukala, J. Appl. Phys. **76**, 1665 (1994).

[8] J. R. Sootsman, D. Y. Chung, and M. G. Kanatzidis, Angew. Chem., Int. Ed. **48**, 8616 (2009).

[9] R. P. Hermann, F. Grandjean, and G. J. Long, Am. J. Phys. **73**, 110 (2005).

[10] V. Keppens, D. Mandrus, B. C. Sales, B. C. Chakoumakos, P. Dai, R. Coldea, M. B. Maple, D. A. Gajewski, E. J. Freeman, and S. Bennington, Nature (London) **395**, 876 (1998).

[11] M. M. Koza, M. R. Johnson, R. Viennois, H. Mutka, L. Girard, and D. Ravot, Nature Mater. **7**, 805 (2008).

[12] G. P. Meisner, D. T. Morelli, S. Hu, J. Yang, and C. Uher, Phys. Rev. Lett. **80**, 3551 (1998).

[13] D. T. Morelli, G. P. Meisner, B. X. Chen, S. Q. Hu, and C. Uher, Phys. Rev. B **56**, 7376 (1997).

[14] K. Ohno, K. Esfarjani, and Y. Kawazoe, *Computational Materials Science: From ab initio to Monte Carlo Methods*, Solid State Series Vol. 129 (Springer-Verlag, Berlin, Germany, 1999), Appendix B.

[15] P. G. Klemens, Int. J. Thermophys. **22**, 265 (2001).

[16] N. Bernstein, J. L. Feldman, and D. J. Singh, Phys. Rev. B **81**, 134301 (2010).

[17] K. Matsuhira *et al.*, J. Phys. Soc. Jpn. **78**, 124601 (2009).

[18] C. Godart, A. P. Gonçalves, E. B. Lopes, and B. Villeroy, *Properties and Applications of Thermoelectric Materials* (Springer, Netherlands, 2009).

[19] B. C. Sales *et al.*, J. Solid State Chem. **146**, 528 (1999).

[20] W. Schnelle, A. Leithe-Jasper, H. Rosner, R. Cardoso-Gil, R. Gumeniuk, D. Trots, J. A. Mydosh, and Y. Grin, Phys. Rev. B **77**, 094421 (2008).

[21] D. Wee, B. Kozinsky, N. Marzari, and M. Fornari, Phys. Rev. B **81**, 045204 (2010).

[22] B. Poudel, Q. Hao, Y. Ma, Y. C. Lan, A. Minnich, B. Yu, X. Yan, D. Z. Wang, A. Muto, D. Vashaee, X. Chen, J. Liu, M. S. Dresselhaus, G. Chen, and Z. F. Ren, Science **320**, 634 (2008).

[23] G. Joshi, H. Lee, Y. C. Lan, X. Wang, G. Zhu, D. Z. Wang, R. W. Gould, D. C. Cuff, M. Y. Tang, M. S. Dresselhaus, G. Chen, and Z. F. Ren, Nano Lett. **8**, 4670 (2008).

[24] X. W. Wang, H. Lee, Y. C. Lan, G. H. Zhu, G. Joshi, D. Z. Wang, J. Yang, A. J. Muto, M. Y. Tang, J. Klatsky, S. Song, M. S. Dresselhaus, G. Chen, and Z. F. Ren, Appl. Phys. Lett. **93**, 193121 (2008).

[25] G. H. Zhu, H. Lee, Y. C. Lan, X. W. Wang, G. Joshi, D. Z. Wang, J. Yang, D. Vashaee, H. Guilbert, A. Pillitteri, M. S. Dresselhaus, G. Chen, and Z. F. Ren, Phys. Rev. Lett. **102**, 196803 (2009).

[26] J. Yang, Q. Hao, H. Wang, Y. C. Lan, Q. Y. He, A. J. Minnich, D. Z. Wang, J. A. Harriman, V. M. Varki, M. S. Dresselhaus, G. Chen, and Z. F. Ren, Phys. Rev. B **80**, 115329 (2009).

[27] R. Giri, N. Yanase, C. Sekine, I. Shirotani, I. Inagawa, C. H. Lee, A. Yamamoto, H. Obara, and T. Yagi, *La doping effect in thermoelectric properties of skutterudite compound* $CeRu_4 P_{12}$, Proceedings ICT 2002. Twenty-First International Conference on Thermoelectrics, (IEEE, Piscataway, NJ, 1997), pp. 60–63.

[28] A. Watcharapasorn, R. C. DeMattei, R. S. Feigelson, T. Caillat, A. Borshchevsky, G. J. Snyder, and J. P. Fleurial, J. Appl. Phys. **86**, 6213 (1999).

[29] A. Watcharapasorn, R. S. Feigelson, T. Caillat, A. Borshchevsky, G. J. Snyder, and J. P. Fleurial, J. Appl. Phys. **91**, 1344 (2002).